# A Bivariate Spline Approach for Image Enhancement

Qianying Hong *and Ming-Jun Lai †
Department of Mathematics
The University of Georgia
Athens, GA 30602

November 7, 2010

**Abstract**

A new approach for image enhancement is developed in this paper. It is based on bivariate spline functions. By choosing a local region from an image to be enhanced, one can use bivariate splines with minimal surface area to enhance the image by reducing noises, smoothing the contrast, e.g. wrinkles and removing stains or damages from images. To establish this approach, we first discuss its mathematical aspects: the existence, uniqueness and stability of the splines of minimal surface area and propose an iterative algorithm to compute the fitting splines of minimal surface area. The convergence of the iterative solutions will be established. In addition, the fitting splines of minimal surface area are convergent as the size of triangulation goes to zero for image functions in $W^{1,1}$. Finally, several numerical examples are shown to demonstrate the effectiveness of this new approach.

## 1 Introduction

In this paper we propose to use bivariate splines to approximate the minimizer of the well-known ROF model for image denoising:

$$\min_{u\in BV(\Omega)} |u|_{BV} + \frac{1}{2\lambda}\int_\Omega |u-f|^2, \tag{1}$$

where $BV(\Omega)$ stands for the space of all functions of bounded variation over $\Omega$, $|u|_{BV}$ denotes the semi-norm in $BV(\Omega)$, and $f$ is a given noised image. As a by-product, we propose a new spline method for scattered data fitting by approximating the minimizer above based on discrete noised image values.

The minimization in (1) has been studied for about twenty years. See [ROF'92], [Acar and Vogel'94], [Chambolle and Lions'97], [Aubert and Kornprobst'06], [Chambolle'04], [Duval, Aujol and Vesse'09], and many references in [Tai'09]. Many numerical methods have been proposed to approximate the minimizer. Typically, one first regularizes the minimization by considering the following $\epsilon$-version of the ROF model:

$$\min_{u\in BV(\Omega)} \int_\Omega \sqrt{\epsilon + |\nabla u|^2} + \frac{1}{2\lambda}\int_\Omega |u-f|^2, \tag{2}$$

where $\nabla u$ is the standard gradient of $u$. Here the first integral is well defined for $u \in W^{1,1}(\Omega)$ which is dense in $BV(\Omega)$. But for $u \in BV(\Omega)\backslash W^{1,1}(\Omega)$, we use Acar and Vogel's equivalent formula (cf. [Acar and Vogel'94]). In addition to the prime and dual algorithm (cf. [Chambolle'04]) and projected gradient algorithm (cf. [Duval, Aujol and Vesse'09]) to numerically solve the minimizer of (1) directly, finite

*qyhong@math.uga.edu
†mjlai@math.uga.edu. This author is partly supported by the National Science Foundation under grant DMS-0713807

difference and finite element methods have been used for numerical solution of (2) by solving its Euler-Lagrange equation

$$\text{div}\ \left(\frac{\nabla u}{\sqrt{\epsilon+|\nabla u|^2}}\right)-\frac{1}{\lambda}(u-f)=0 \tag{3}$$

or its time dependent version

$$u_t=\text{div}\ \left(\frac{\nabla u}{\sqrt{\epsilon+|\nabla u|^2}}\right)-\frac{1}{\lambda}(u-f) \tag{4}$$

starting with $u(x,y,0)=u_0$ together with Dirichlet or Neumann boundary condition. We refer to [Vogel and Oman'96], [Dobson and Vogel'97], [Feng and Prohl'03], and [Feng, Oehsen, and Prohl'05] for theoretical studies of finite difference and finite element methods.

Let $\triangle$ be a triangulation of $\Omega$. Fix $r\geq 0$ and $d>r$. Let $C^r(\Omega)$ be the class of all $r$th continuously differentiable functions over $\Omega$ and

$$S_d^r(\triangle)=\{s\in C^r(\Omega),\quad s|_t\in\mathcal{P}_d,\forall t\in\triangle\}$$

be the spline space of degree $d$ and smoothness $r$ over triangulation $\triangle$, where $\mathcal{P}_d$ is the space of all polynomials of degree $\leq d$ and $t$ is a triangle in $\triangle$. For properties of bivariate splines, see [Lai and Schumaker'07]. As an image may not be very smooth over $\Omega$, we mainly use $r=0$ and $d=1$ or $r=1, d\geq 3$. For convenience, let $\mathcal{S}$ be one of these spline spaces $S_d^r(\triangle)$ for a fixed $r$ and fixed $d$ with $d>r$. We shall explain how to use these functions to approximate the minimizer of (2) in this paper.

To authors' knowledge, bivariate splines have not been used to solve the nonlinear PDE (3) nor time dependent PDE (4) in the literature so far. Let us describe our spline approach more precisely. We first select a polygonal region $\Omega$ of interest from a standard image domain $[1,512]\times[1,512]$, partition $\Omega$ into a triangulation $\triangle$, use bivariate splines in $\mathcal{S}$ to find a fitting spline with surface area minimized, and finally replace the image values over $\Omega$ by the spline values so that the image over $\Omega$ is smooth and less vibrations/oscillations. Heuristically, the noises and stains cause the bumpiness of the fitting spline surfaces. Minimizing the surface area of the fitting spline function will reduce the bumpiness and hence, reduce the noises, remove the stains so that the image is enhanced. As the domain is a polygon with arbitrarily geometric shape, bivariate splines are much more convenient than tensor products of B-splines in this situation. Thus, we restrict our discussion to bivariate splines in this paper.

Clearly, bivariate splines extend continuous linear finite elements. Thus our approach generalizes the numerical methods in [Dobson and Vogel'96] and [Feng and Prohl'03]. Let us describe our results in this paper. For convenience, let $\epsilon=1$. It is known that the following minimization

$$\min\{E(u),\quad u\in BV(\Omega)\}, \tag{5}$$

where the energy functional $E(u)$ is defined by

$$E(u)=\int_\Omega\sqrt{1+|\nabla u|^2}dx+\frac{1}{2\lambda}\frac{1}{A_\Omega}\int_\Omega|u-f|^2dx \tag{6}$$

has a unique solution, where $A_\Omega$ is the area of polygonal domain $\Omega$. We use $u_f$ to denote the minimizer. The discussion of the existence and uniqueness of the minimizer of (5) can be found in [Acar and Vogel'94] and [Chambolle and Lions'97]. Similarly, we know that

$$\min\{E(u),\quad u\in\mathcal{S}(\triangle)\}, \tag{7}$$

has a unique solution. We shall denote by $S_f$ the minimizer of (7). One of our main results is to show

**Theorem 1.1** *Suppose $\Omega$ is a bounded domain with Lipschitz boundary. Suppose that $\triangle$ is a $\beta$-quasi-uniform triangulation of $\Omega$. If $u_f \in W^{1,1}(\Omega)$, then $S_f$ converges to $u_f$ in $L^2(\Omega)$ norm as the size $|\triangle|$ of triangulation $\triangle$ goes to zero. More precisely,*

$$\|S_f - u_f\|_{L^2(\Omega)} \to 0, \quad \text{when } |\triangle| \to 0,$$

*where $|\triangle|$ denotes the size of triangulation $\triangle$ to be defined in the next section. When $u_f \in W^{1,2}(\Omega)$,*

$$\|S_f - u_f\|_{L^2(\Omega)} \le C\sqrt{|\triangle|}$$

*for a positive constant $C$ independent of $\triangle$.*

Next we shall discuss how to compute the minimizer $S_f$ of (7). First the minimizer $S_f$ satisfies the following nonlinear equations: letting $\{\phi_1, \cdots, \phi_N\}$ be a basis for $\mathcal{S}$,

$$\frac{\partial}{\partial t} E(S_f + t\phi_j, f)\big|_{t=0} = \int_\Omega \frac{\nabla S_f \cdot \nabla \phi_j}{\sqrt{1+|\nabla S_f|^2}} dx + \frac{1}{\lambda}\frac{1}{A_\Omega}\int_\Omega (S_f - f)\phi_j dx = 0 \tag{8}$$

for all basis functions $\phi_j, j = 1, \cdots, N$. As these are nonlinear equations, we will use a fixed point iterative algorithm as in [Dobson and Vogel'96]. Our next result is to show the convergence of the iterative algorithm. Our analysis is completely different from the one given in [Dobson and Vogel'96].

Finally, in practice, we are given discrete noised image values over $\Omega$. That is, we have $\{(x_i, f_i), i = 1, \cdots, n\}$ with $x_i \in \Omega$ and noised function values $f_i$ for $i = 1, \cdots, n$. Let

$$E_d(u) = \int_\Omega \sqrt{1+|\nabla u(x)|^2} dx + \frac{1}{2\lambda}\frac{1}{n}\sum_{i=1}^n |u(x_i) - f_i|^2 \tag{9}$$

be an energy functional based on the discrete noised image values. We use bivariate splines to solve the following minimization problem:

$$\min\{E_d(u), \quad u \in \mathcal{S}\}. \tag{10}$$

It is easy to see that $E_d$ is a convex functional. However, it is not strictly convex. As $\mathcal{S}$ is a finite dimensional space, the above problem (10) will have a solution. However, it may not be unique unless the data locations satisfy some conditions. Thus, we shall explain such conditions to ensure the uniqueness. It is known that there are discrete least squares splines and penalized least squares splines available in the literature which can be used to reduce the noises from the data values. See a survey paper [Lai08] on multivariate splines for data fitting. Similar to (8), the Euler-Lagrange equations for (10) are nonlinear and we use the fixed point iterative algorithm to find the minimizers. We shall use the penalized least squares spline of the noised data as an initial guess for the iterative algorithm and do several iterations to further reduce the bumpiness and/or oscillations of the fitting surface. Hence this leads to a new spline method for data fitting and it will have a better performance than standard discrete and penalized least squares splines for reducing noises, removing wrinkles and hence enhancing images.

Let us summarize our discussion above. Essentially, our bivariate spline approach is a local method. If we want to remove stains, we select a local domain containing a stain and then compute a fitting spline to remove it. As demonstrated in numerical examples in Section 5, if we want to de-noise an image, we reduce noises from many local domains separately instead of denoising the entire image at once. In particular, we propose a two-stage method for image denoising. That is, we first use a favorable algorithm, e.g. Chambolle algorithm (cf. [Chambolle'04]) or a finite difference solution of the Perona-Malik diffusive PDE (cf. [Perona-Malik'90] or [Aubert and Kornprobst'06]) to remove noises. We then choose some regions of interest from the de-noised image and apply our bivariate spline approach to further reduce noises over these interested regions.

The paper is organized as follows. We begin with a preliminary section on bivariate splines §2. Then we discuss the properties of spline minimizer $S_f$ in detail in §3. Similarly, the properties of the discrete

minimal surface area splines will be contained in §4. Finally in §5 we report our numerical experiments. In particular, we shall explain our image segmentation technique, triangulation technique, and numerical implementation issues on bivariate splines in this section.

# 2 Preliminary

We simply outline some properties of bivariate splines which will be used in later sections. First of all, we need

**Definition 2.1** *Let $\beta < \infty$. A triangulation $\triangle$ is said to be $\beta$-quasi-uniform provided that $|\triangle| \leq \beta\rho_{\triangle}$, where $|\triangle|$ is the maximum of the diameters of the triangles in $\triangle$, and $\rho_{\triangle}$ is the minimum of the radii of the in-circles of triangles of $\triangle$.*

Let $W^{k,p}(\Omega)$ denotes the Sobolev space of local summable functions $u : \Omega \to \mathbb{R}$ such that for each multi-index $\alpha$ with $|\alpha| \leq k$, $D^{\alpha}u$ exists in weak sense and belongs to $L^p(\Omega)$. Let $|f|_{\Omega,m,p}$ denotes the $L_p$ norm of the $m^{th}$ derivatives of $f$ over $\Omega$ that is,

$$|u|_{\Omega,k,p} := \left( \sum_{\nu+\mu=k} \|D_1^{\nu} D_2^{\mu} u\|_{\Omega,p}^p \right)^{1/p}, \quad for\ 1 \leq p < \infty, \tag{11}$$

and $\|f\|_{\Omega,p} = \left( \frac{1}{A_\Omega} \int_\Omega |f(x)|^q dx \right)^{1/p}$ be the standard $L^p(\Omega)$ norm.

We first use the so-called Markov inequality to compare the size of the derivative of a polynomial with the size of the polynomial itself on a given triangle $t$. (See [22] for a proof. )

**Theorem 2.1** *Let $t := \langle v_1, v_2, v_3 \rangle$ be a triangle, and fix $1 \leq q \leq \infty$. Then there exists a constant $K$ depending only on $d$ such that for every polynomial $p \in \mathcal{P}_d$, and any nonnegative integers $\alpha$ and $\beta$ with $0 \leq \alpha + \beta \leq d$,*

$$\|D_1^{\alpha} D_2^{\beta} p\|_{q,t} \leq \frac{K}{\rho_t^{\alpha+\beta}} \|p\|_{q,t}, \quad 0 \leq \alpha + \beta \leq d, \tag{12}$$

*where $\rho_t$ denotes the radius of the largest circle inscribed in $t$.*

Next we have the following approximation property (cf. [21] and [22]):

**Theorem 2.2** *Assume $d \geq 3r+2$ and let $\triangle$ be a triangulation of $\Omega$. Then there exists a quasi-interpolatory operator $Qf \in S_d^r(\triangle)$ mapping $f \in L_1(\Omega)$ into $S_d^r(\triangle)$ such that $Qf$ achieves the optimal approximation order: if $f \in W^{m+1,p}(\Omega)$,*

$$\|D_1^{\alpha} D_2^{\beta} (Qf - f)\|_{\Omega,p} \leq C|\triangle|^{m+1-\alpha-\beta} |f|_{\Omega,m+1,p} \tag{13}$$

*for all $\alpha + \beta \leq m+1$ with $0 \leq m \leq d$. Here the constant $C$ depends only on the degree $d$ and the smallest angle $\theta_{\triangle}$ and may be dependent on the Lipschitz condition on the boundary of $\Omega$.*

Bivariate splines have been used for data fitting for a long time. Theoretical results on the existence, uniqueness and approximation as well as numerical computational algorithms and experiments are well known (cf. [2], [17], [18], [19], and [20]). Let us present a brief summary. Let $s_{0,f} \in \mathcal{S}$ be the spline satisfying

$$\mathcal{L}(s_{0,f} - f) = \min\{\mathcal{L}(s - f), \quad s \in \mathcal{S}\}. \tag{14}$$

where $\mathcal{L}(s-f) = \dfrac{1}{n}\sum_{i=1}^{n}|s(x_i)-f_i|^2$. $s_{0,f}$ is called the least squares spline of $f$. Another data fitting method is called penalized least squares spline method. Letting

$$E_m(f) = \frac{1}{A_\Omega}\int_\Omega \sum_{i+j=m}\left(\binom{m}{i}(D_1^i D_2^j f)^2\right)dx_1dx_2$$

be the energy functional, and $\lambda > 0$ be a fixed real number, we let $s_{\lambda,f} \in \mathcal{S}$ be the spline solving the following minimization problem:

$$\min_{s\in\mathcal{S}} \mathcal{L}(s-f) + \lambda E_m(s) \tag{15}$$

for a fixed integer $m = 2$.

Suppose that the data locations $\mathcal{V} = \{x_i, i = 1, \cdots, n\}$ have the property that for every $s \in \mathcal{S}$ and every triangle $\tau \in \triangle$, there exist a positive constant $F_1$, independent of $s$ and $\tau$, such that

$$F_1\|s\|_{\infty,\tau} \le (\sum_{v\in\mathcal{V}\cap\tau} s(v)^2)^{1/2}. \tag{16}$$

Let $F_2$ be the largest number of data sites in a triangle $\tau \in \triangle$. That is, we have

$$\left\{\sum_{v\in\mathcal{V}\cap\tau} s(v)^2\right\}^{1/2} \le F_2\|s\|_{\infty,\tau}, \tag{17}$$

where $\|s\|_{\infty,\tau}$ denotes the maximum norm of $s$ over domain $\tau$.

The approximation properties of the discrete and penalized least squares splines are known (cf. [18], [19], and [20]).

**Theorem 2.3** *Suppose that $d \ge 3r+2$ and $\triangle$ is a $\beta$ quasi-uniform triangulation. Suppose that there exist two positive constants $F_1$ and $F_2$ such that (16) and (17) are satisfied. Then there exists a constant $C$ depending on $d$ and $\beta$ such that for every function $f$ in Sobolev space $W^{m+1,\infty}(\Omega)$ with $1 \le m \le d$ such that*

$$\|f - s_{\lambda,f}\|_{\infty,\Omega} \le C\frac{F_2}{F_1}|\triangle|^{m+1}|f|_{m+1,\infty,\Omega} + \frac{\lambda}{(F_1^2|\triangle|)}C|f|_{2,\infty,\Omega}$$

*for $0 < \lambda \le F_1|\triangle|^2/\beta^2$. In particular, when $\lambda = 0$, we have*

$$\|f - s_{0,f}\|_{\infty,\Omega} \le C\frac{F_2}{F_1}|\triangle|^{m+1}|f|_{m+1,\infty,\Omega}. \tag{18}$$

*Here $m$ is an integer between 0 and $d$.*

# 3 Spline Minimizer $S_f$ and Its Properties

Recall that $S_f$ is the solution to the minimization problem (7) and $u_f$ is the solution to (5). The existence of these solutions were explained in the Introduction. We shall show that the minimization (7) is stable and the spline minimizer $S_f$ converges to $u_f$ as the size of triangulation goes to zero.

## 3.1 Stability of the Minimization (7)

In this subsection we shall show that the minimization is stable

**Lemma 3.1** *Suppose we have another function $g \in L^2(\Omega)$. Let $S_g \in \mathcal{S}$ be the minimizer of (7) associated with $g$. Then the norm of the difference of $S_f$ and $S_g$ is bounded by the norm of the difference of $f$ and $g$, i.e.*

$$\|S_f - S_g\|_2 \leq \|f - g\|_2. \tag{19}$$

**Proof.** For more precise, we let

$$E(u, f) := \int_\Omega \sqrt{1 + |\nabla u|^2} dx + \frac{1}{2\lambda A_\Omega} \int_\Omega |u - f|^2 dx$$

and similar for $E(u, g)$. It is clear that $E(u, f)$ is Frechet differentiable with respect to $u$. The uniqueness of $S_f$ and $S_g$ implies that all directional derivatives of $E(u, f)$ and $E(u, g)$ in (8) vanish in the space of finite dimensional space $\mathcal{S}$ spanned by $\phi_j$, $j = 1, ..., n$. That is,

$$\frac{\partial}{\partial t} E(S_f + t\phi_j, f)|_{t=0} = \int_\Omega \frac{\nabla S_f \cdot \nabla \phi_j}{\sqrt{1 + |\nabla S_f|^2}} dx + \frac{1}{\lambda} \frac{1}{A_\Omega} \int_\Omega (S_f - f)\phi_j dx = 0 \tag{20}$$

$$\frac{\partial}{\partial t} E(S_g + t\phi_j, g)|_{t=0} = \int_\Omega \frac{\nabla S_g \cdot \nabla \phi_j}{\sqrt{1 + |\nabla S_g|^2}} dx + \frac{1}{\lambda} \frac{1}{A_\Omega} \int_\Omega (S_g - g)\phi_j dx = 0 \tag{21}$$

Subtracting (21) from (20), we have,

$$\int_\Omega \frac{\nabla S_f \cdot \nabla \phi_j}{\sqrt{1 + |\nabla S_f|^2}} - \frac{\nabla S_g \cdot \nabla \phi_j}{\sqrt{1 + |\nabla S_g|^2}} dx + \frac{1}{\lambda} \frac{1}{A_\Omega} \int_\Omega (S_f - S_g)\phi_j dx = \frac{1}{\lambda} \frac{1}{A_\Omega} \int_\Omega (f - g)\phi_j dx. \tag{22}$$

Since $S_f$ and $S_g$ are in the finite dimensional space $\mathcal{S}$, we can write $S_f - S_g = \sum_{j=1}^{n} c_j \phi_j$ for some coefficients $c_j$. Thus $\sum_{j=1}^{n} c_j \nabla \phi_j = \nabla(S_f - S_g)$. Multiply $c_j$ to (22) for each $j$ and sum them up from $j = 1, \cdots, n$. We get

$$\begin{aligned} & \lambda \int_\Omega \left( \frac{\nabla S_f}{\sqrt{1 + |\nabla S_f|^2}} - \frac{\nabla S_g}{\sqrt{1 + |\nabla S_g|^2}} \right) \cdot \nabla(S_f - S_g) dx + \frac{1}{A_\Omega} \int_\Omega |S_f - S_g|^2 dx \\ = & \quad \frac{1}{A_\Omega} \int_\Omega (f - g)(S_f - S_g) dx. \end{aligned} \tag{23}$$

Notes that $\rho(t) = \sqrt{1 + |t|^2}$ is a convex differentiable multivariate function for $t \in \mathbf{R}^2$, where $|t|$ stands for the norm of vector $t$. Its Hessian matrix $H_\rho(t)$ is not negative. By Taylor expansion, for some $\xi_1$ and $\xi_2$, we have

$$\left( \frac{t_1}{\sqrt{1 + |t_1|^2}} - \frac{t_2}{\sqrt{1 + |t_2|^2}} \right) \cdot (t_1 - t_2) = (t_1 - t_2)^T (H_\rho(\xi_1) + H_\rho(\xi_2))(t_1 - t_2) \geq 0 \tag{24}$$

for any $t_1, t_2 \in \mathbf{R}^2$. In particular, let $t_1 = \nabla S_f$ and $t_2 = \nabla S_g$ in (24). We integrate (24) over $\Omega$ to have

$$\int_\Omega \left( \frac{\nabla S_f}{\sqrt{1 + |\nabla S_f|^2}} - \frac{\nabla S_g}{\sqrt{1 + |\nabla S_g|^2}} \right) \cdot \nabla(S_f - S_g) dx \geq 0. \tag{25}$$

Using the above inequality, the term in (23) becomes

$$\int_\Omega |S_f - S_g)|^2 dx \leq \int_\Omega (f - g)(S_f - S_g) dx$$

Apply Cauchy-Schwarz inequality to the right-hand side of above equation, we have

$$\int_\Omega |S_f - S_g|^2 dx \le \left(\int_\Omega |f-g|^2 dx\right)^{1/2} \left(\int_\Omega |S_f - S_g|^2 dx\right)^{1/2}.$$

The desired inequality (19) follows. These complete the proof. ■

## 3.2 Convergence of $S_f$ to $u_f$

Next we shall show that $S_f$ converges to $u_f$, the minimizer of (5) for the same $\lambda$. Although we can use the arguments in [5] to show the convergence of $S_f$ to $u_f$, the analysis will require $u_f \in W^{2,\infty}(\Omega)$. As an image function may not have such high regularity, we use the following approach to establish the convergence.

**Lemma 3.2** *Let $u_f$ be the solution to (5). For any $u \in BV(\Omega)$,*

$$\|u - u_f\|_2^2 \le 2\lambda A_\Omega (E(u) - E(u_f)). \tag{26}$$

*In particular, we have*

$$\|S_f - u_f\|_2^2 \le 2\lambda A_\Omega (E(S_f) - E(u_f)). \tag{27}$$

**Proof.** Using the concept of sub-differentiation and its basic property (see, e.g. [13]), we have

$$0 = \partial E(u_f) = \partial J(u_f) - \frac{1}{\lambda A_\Omega}(f - u_f) \text{ and } \langle \partial J(u_f), u - u_f\rangle \le J(u) - J(u_f),$$

where $J(u) = \int_\Omega \sqrt{1+|\nabla u|^2}dx$. From the above equations, it follows

$$\frac{1}{\lambda A_\Omega}\int_\Omega (f-u_f)(u-u_f)dx \le \int_\Omega \sqrt{1+|\nabla u|^2} - \sqrt{1+|\nabla u_f|^2}dx. \tag{28}$$

We can write

$$\begin{aligned}
& E(u) - E(u_f) \\
= & \int_\Omega \sqrt{1+|\nabla u|^2} - \sqrt{1+|\nabla u_f|^2}dx + \frac{1}{2\lambda|A_\Omega|}\left(\int_\Omega |u-f|^2dx - \int_\Omega |u_f - f|^2 dx\right) \\
= & \int_\Omega \sqrt{1+|\nabla u|^2} - \sqrt{1+|\nabla u_f|^2}dx + \frac{1}{2\lambda|A_\Omega|}\left(\int_\Omega (u-u_f+u_f-f)^2dx - \int_\Omega |u_f - f|^2 dx\right) \\
= & \int_\Omega \sqrt{1+|\nabla u|^2} - \sqrt{1+|\nabla u_f|^2}dx + \frac{1}{\lambda|A_\Omega|}\int_\Omega (u-u_f)(u_f-f)dx + \frac{1}{2\lambda|A_\Omega|}\int_\Omega |u-u_f|^2dx \\
\ge & \frac{1}{2\lambda|A_\Omega|}\int_\Omega |u-u_f|^2dx
\end{aligned}$$

by (28). Therefore the inequality (26) holds. Hence, we have (27). ■

Next we need to show that $E(S_f) - E(u_f) \to 0$. To this end, we recall two standard concepts. Since $\Omega \subset \mathbb{R}^2$ is an region with piecewise smooth boundary $\partial\Omega$ and $u_f$ is assumed to be in $W^{1,1}(\Omega)$, using the extension theorem in [26], there exists a linear operator $\mathfrak{E} : W^{1,1}(\Omega) \to W^{1,1}(\mathbb{R}^2)$ such that,
(i)$\mathfrak{E}(u_f)|_\Omega = u_f$
(ii)$\mathfrak{E}$ maps $W^{1,1}(\Omega)$ continuously into $W^{1,1}(\mathbb{R}^2)$:

$$\|\mathfrak{E}(u_f)\|_{W^{1,1}(\mathbb{R}^2)} \le C\|u_f\|_{W^{1,1}(\Omega)}. \tag{29}$$

Note that $\mathfrak{E}(u_f)$ is a compactly supported function in $W^{1,1}(\mathbb{R}^2)$. Thus, without loss of generality we may assume $u_f \in W^{1,1}(\mathbb{R}^2)$.

Recall that the standard mollifier $\eta : \mathbb{R}^2 \to \mathbb{R}$ is defined by

$$\eta(x) := \begin{cases} C \exp\left(\frac{1}{|x|^2-1}\right), & if\ |x| < 1 \\ 0, & if\ |x| \geq 1 \end{cases}$$

with the constant $C > 0$ selected so that $\int_{\mathbb{R}^2} \eta(x)dx = 1$. And set

$$\eta_\epsilon(x) := \frac{1}{\epsilon^2}\eta\left(\frac{x}{\epsilon}\right).$$

It is easy to see $\int_{\mathbb{R}^2} \eta_\epsilon(x)dx = 1$, and support$(\eta_\epsilon) \subset B(0,\epsilon)$. Define the mollification $u_f^\epsilon$ of $u_f$ by convolution

$$u_f^\epsilon(x) = \int_{\Omega_\epsilon} \eta_\epsilon(x-y)u_f(y)dy = \int_{B(x,\epsilon)} \eta_\epsilon(x-y)u_f(y)dy,$$

where $\Omega_\epsilon := \{x \in \mathbb{R}^2 \mid \text{dist}(x,\Omega) < \epsilon\}$. It is known that $\|u_f^\epsilon - u_f\|_2 \to 0$ as $\epsilon \to 0$ and $u_f^\epsilon \in C_0^\infty(\Omega_\epsilon)$. See, e.g. [14]. In particular, when $u_f \in W^{1,2}(\Omega)$, we have

$$\|u_f^\epsilon - u_f\|_2 \leq C|u_f|_{W^{1,2}(\Omega)}\epsilon \tag{30}$$

for a positive constant $C$ independent of $\epsilon$ and $f$.

Our general plan to show $E(S_f) - E(u_f) \to 0$ is to establish the following sequence of inequalities:

$$E(u_f) \leq E(S_f) \leq E(Qu_f^\epsilon) \leq E(u_f^\epsilon) + \text{err}(|\triangle|,\epsilon) \leq E(u_f) + \text{err}_\epsilon + \text{err}(|\triangle|,\epsilon),$$

where $Qu_f^\epsilon$ is a spline approximation of $u_f^\epsilon$ as in Theorem 2.2 and $\text{err}(|\triangle|,\epsilon)$ and $\text{err}_\epsilon$ are error terms which will go to zero when $\epsilon$ and $|\triangle|$ go to zero.

We first show $E(u_f^\epsilon)$ approximates $E(u_f)$.

**Lemma 3.3** *Let $u_f^\epsilon$ be the mollification of $u_f$ defined above. Then $E(u_f^\epsilon)$ approximates $E(u_f)$, when $\epsilon \to 0$. In particular, when $u_f \in W^{1,2}(\Omega), E(u_f^\epsilon) - E(u_f) \leq C\epsilon$ for a positive constant dependent on $u_f$.*

**Proof.** First we claim that

$$E(u_f^\epsilon) \leq E(u_f) + err_\epsilon$$

for an error term $err_\epsilon$

$$err_\epsilon = \int_{\Omega_\epsilon \setminus \Omega} \sqrt{1+|\nabla u_f(y)|^2}dy + \frac{1}{2\lambda}\left(\|u_f^\epsilon - u_f\|_2^2 + 2\|u_f^\epsilon - u_f\|_2 \|u_f - f\|_2\right) \tag{31}$$

which will be shown to go to zero when $\epsilon \to 0$ below.

By the convexity of $\sqrt{1+|t|^2}$ and the property of the mollifier, we have

$$\sqrt{1+|\nabla u_f^\epsilon(x)|^2} = \sqrt{1+\left|\int_{B(0,\epsilon)} \eta_\epsilon(x-y)\nabla u_f(y)dy\right|^2} \leq \int_{B(x,\epsilon)} \eta_\epsilon(x-y)\sqrt{1+|\nabla u_f(y)|^2}dy.$$

It follows that

$$\begin{aligned} \int_\Omega \sqrt{1+|u_f^\epsilon(x)|^2}dx &\leq \int_\Omega \int_{B(x,\epsilon)} \eta_\epsilon(x-y)\sqrt{1+|\nabla u_f(y)|^2}dydx. \\ &\leq \int_{\Omega_\epsilon} \sqrt{1+|\nabla u_f(y)|^2} \int_{B(y,\epsilon)} \eta_\epsilon(x-y)dxdy \\ &= \int_{\Omega_\epsilon} \sqrt{1+|\nabla u_f(y)|^2}dy. \\ &= \int_\Omega \sqrt{1+|\nabla u_f(y)|^2}dy + \int_{\Omega_\epsilon \setminus \Omega} \sqrt{1+|\nabla u_f(y)|^2}dy. \end{aligned}$$

By $u_f \in W^{1,1}(\mathbb{R}^2)$ and (29), it follows that

$$\int_{\Omega_\epsilon \setminus \Omega} \sqrt{1+|\nabla u_f(y)|^2} dy \le \int_{\Omega_\epsilon \setminus \Omega} (1+|\nabla u_f(y)|)\, dy \to 0, \quad as\ \epsilon \to 0.$$

Next we have

$$\frac{1}{2\lambda}\|u_f^\epsilon - f\|_2^2 \le \frac{1}{2\lambda}\left(\|u_f^\epsilon - u_f\|_2^2 + 2\|u_f^\epsilon - u_f\|_2\|u_f - f\|_2 + \|u_f - f\|_2^2\right).$$

Since $\|u_f^\epsilon - u_f\|_2 \to 0$ as explained above and $\|u_f - f\|_2$ is bounded because $\frac{1}{2\lambda}\|u_f - f\|^2 \le E(0)$,

$$\frac{1}{2\lambda}\left(\|u_f^\epsilon - u_f\|_2^2 + 2\|u_f^\epsilon - u_f\|_2\|u_f - f\|_2\right) \to 0, \quad as\ \epsilon \to 0.$$

This finishes the proof of our claim.

Clearly, $u_f^\epsilon \in W^{1,1}(\Omega) \subset BV(\Omega)$. As $u_f$ is the minimizer in $BV(\Omega)$, it follows that

$$E(u_f) \le E(u_f^\epsilon) \le E(u_f) + err_\epsilon,$$

which implies $E(u_f^\epsilon)$ approximates $E(u_f)$ when $\epsilon \to 0$.

When $u_f \in W^{1,2}(\Omega)$, the above analysis applies. Together with (30), we use (31) to conclude

$$err_\epsilon \le C|u_f|_{W^{1,2}(\Omega)}\epsilon.$$

■

We next estimate $E(Qu_f^\epsilon) - E(u_f^\epsilon)$. To do so, we need semi-norm $|u_f^\epsilon|_{W^{2,1}(\Omega_\epsilon)}$.

**Lemma 3.4** *For any fixed $\epsilon > 0$, $u_f^\epsilon \in W^{2,1}(\Omega_\epsilon)$ and*

$$|u_f^\epsilon|_{W^{2,1}(\Omega_\epsilon)} \le \frac{C}{\epsilon}|u_f|_{W^{1,1}(\Omega)} \tag{32}$$

*for a constant $C > 0$.*

**Proof.** Due to the mollification, $u_f^\epsilon \in W^{2,1}(\Omega_\epsilon)$. Letting $D_1$ denote the partial derivative with respect to the first variable, we consider $\|D_1 D_1 u_f^\epsilon\|_{L^1(\Omega_\epsilon)}$. Recall that $u_f^\epsilon(x) = \int_{B(x,\epsilon)} \eta_\epsilon(x-y)u_f(y)dx$. We have

$$D_1 D_1 u_f^\epsilon = -\int_{B(x,\epsilon)} D_1 u_f(y) D_1 \eta_\epsilon(x-y) dy.$$

It follows that

$$\begin{aligned}
|D_1 D_1 u_f^\epsilon|_{L^1(\Omega_\epsilon)} &= \int_{\Omega_\epsilon} \left| \int_{B(x,\epsilon)} D_1 u_f(y) D_1 \eta_\epsilon(x-y) dy \right| dx \\
&\le \int_{\Omega} \int_{B(x,\epsilon)} |D_1 u_f(y)||D_1 \eta_\epsilon(x-y)| dy dx \\
&\le \int_{\Omega_\epsilon} |D_1 u_f(y)| \int_{B(y,\epsilon)} |D_1 \eta_\epsilon(x-y)| dx dy \\
&= \int_{\Omega_\epsilon} |D_1 u_f(y)| dy \int_{B(0,\epsilon)} |D_1 \eta_\epsilon(x)| dx.
\end{aligned}$$

Since

$$|D_1\eta_\epsilon(x)| \leq \frac{8C\exp(-2)}{\epsilon^3},$$

we have

$$|D_1D_1u_f^\epsilon|_{L^1(\Omega_\epsilon)} \leq \|D_1u_f\|_{L^1(\Omega)}\frac{C\exp(-2)}{\epsilon^3}\int_{B(0,\epsilon)}dx \leq |u_f|_{W^{1,1}(\Omega)}\frac{C'}{\epsilon} \tag{33}$$

for a positive constant $C'$. Using the similar arguments, we can show that $\|D_1D_2u_f^\epsilon\|_{L^1(\Omega_\epsilon)}$ and $\|D_2D_2u_f^\epsilon\|_{L^1(\Omega_\epsilon)}$ have the same upper bound as in (33). And thus, we prove that

$$|u_f^\epsilon|_{W^{2,1}(\Omega_\epsilon)} \leq \frac{C}{\epsilon}|u_f|_{W^{1,1}(\Omega)}$$

for another positive constant $C > 0$. ■

Recall $\triangle$ is a triangulation of $\Omega$. Let $\triangle' = \{t_i\}$ be a new triangulation of $\Omega_\epsilon$ with $\triangle \subset \triangle'$ and $|\triangle'| = |\triangle|$. Using Theorem 2.2, we can choose $Qu_f^\epsilon \in \mathcal{S}(\triangle')$ such that

$$\|D_1^\alpha D_2^\beta(Q(u_f^\epsilon) - u_f^\epsilon)\|_{L^1(\Omega_\epsilon)} \leq C|\triangle|^{2-\alpha-\beta}|u_f^\epsilon|_{W^{2,1}(\Omega_\epsilon)} \tag{34}$$

for all $\alpha + \beta = 1$.

**Lemma 3.5** *Let $\tilde{s} := Qu_f^\epsilon|_\Omega$ be the restriction of $Qu_f^\epsilon$ on $\Omega$ which is a spline in $\mathcal{S}$. Then $E(\tilde{s})$ approximates $E(u_f^\epsilon)$, when $\frac{|\triangle|}{\epsilon} \to 0$.*

**Proof.** We first estimate the difference between $|E(\tilde{s}) - E(u_f^\epsilon)|$ by

$$\begin{aligned}
& |E(\tilde{s}) - E(u_f^\epsilon)| \\
\leq\ & \left|\int_\Omega \sqrt{1+|\nabla\tilde{s}|^2} - \sqrt{1+|\nabla u_f^\epsilon|^2}dx\right| + \frac{1}{2\lambda}\left|\|\tilde{s}-f\|_2^2 - \|u_f^\epsilon - f\|_2^2\right| \\
\leq\ & \left|\int_\Omega \sqrt{1+|\nabla\tilde{s}|^2} - \sqrt{1+|\nabla u_f^\epsilon|^2}dx\right| + \frac{1}{2\lambda}\left(\|\tilde{s}-u_f^\epsilon\|_2^2 + 2\|\tilde{s}-u_f^\epsilon\|_2\,\|u_f^\epsilon - f\|_2\right).
\end{aligned}$$

Let $err(|\triangle|,\epsilon)$ be the term on the right-hand side of the inequality above. Let us show that $err(|\triangle|,\epsilon) \to 0$, as $|\triangle|/\epsilon \to 0$. Note that $Q(u_f^\epsilon)$ is supported over $\Omega_\epsilon$ by the construction of quasi-interpolatory operator $Q$.

$$\|\nabla(\tilde{s}-u_f^\epsilon)\|_{L^1(\Omega)} \leq \|\nabla(Q(u_f^\epsilon)-u_f^\epsilon)\|_{L^1(\Omega_\epsilon)} \leq C|\triangle'||u_f^\epsilon|_{W^{2,1}(\Omega_\epsilon)} \leq \frac{C|\triangle|}{\epsilon}|u_f|_{W^{1,1}(\Omega)} \tag{35}$$

by using the inequality in (34) with $\alpha+\beta=1$. Hence, we have

$$\begin{aligned}
& \left|\int_\Omega \sqrt{1+|\nabla\tilde{s}|^2} - \sqrt{1+|\nabla u_f^\epsilon|^2}dx\right| = \left|\int_\Omega \frac{|\nabla\tilde{s}|^2 - |\nabla u_f^\epsilon|^2}{\sqrt{1+|\nabla\tilde{s}|^2}\sqrt{1+|\nabla u^{\epsilon_f}|^2}}dx\right| \\
\leq\ & \int_\Omega \frac{|\nabla\tilde{s}-\nabla u_f^\epsilon||\nabla\tilde{s}+\nabla u_f^\epsilon|}{\sqrt{1+|\nabla\tilde{s}|^2}\sqrt{1+|\nabla u_f^\epsilon|^2}}dx \\
\leq\ & \|\nabla(\tilde{s}-u_f^\epsilon)\|_{L^1(\Omega)} \\
\leq\ & C'\frac{|\triangle|}{\epsilon}|u_f|_{W^{1,1}(\Omega)}.
\end{aligned}$$

Here both $C$ and $C'$ are positive constants independent of $\epsilon, \triangle, u_f$.

It is not hard to see the quantity $\|u_f^\epsilon - f\|_2$ is bounded because

$$\|u_f^\epsilon - f\|_2 \leq \|u_f^\epsilon - u_f\|_2 + \|u_f - f\|_2 \leq 1 + \sqrt{2\lambda A_\Omega}\|f\|_2$$

as $\|u_f^\epsilon - u_f\|_2 \le 1$ if $\epsilon$ small enough and by using the property of the minimizer $u_f$. By using the well-known Sobolev inequality: for any function $g \in W^{1,1}(\Omega_\epsilon)$,

$$\|g\|_{L^2(\Omega_\epsilon)} \le C|\nabla g|_{L^1(\Omega_\epsilon)}$$

for $\Omega_\epsilon$ with $C^1$ boundary (cf. [14]), we have,

$$\|\tilde{s} - u_f^\epsilon\|_{L^2(\Omega)} \le \|\tilde{s} - u_f^\epsilon\|_{L^2(\Omega_\epsilon)} \le C\|\nabla(\tilde{s} - u_f^\epsilon)\|_{L^1(\Omega_\epsilon)} \le \frac{C|\triangle|}{\epsilon}|u_f|_{W^{1,1}(\Omega)}$$

by (35). Therefore, we conclude that $err(|\triangle|, \epsilon) \to 0$, as $|\triangle|/\epsilon \to 0$, and thus $E(\tilde{s})$ approximates $E(u_f^\epsilon)$. ■

Summarizing the discussion above, we have

**Theorem 3.1** *Suppose that $u_f \in W^{1,1}(\Omega)$. Then $S_f$ approximates $u_f$ in $L^2(\Omega)$ when $|\triangle| \to 0$. In particular, when $u_f \in W^{1,2}(\Omega)$,*

$$\|S_f - u_f\|_2 \le C|u_f|_{W^{1,2}(\Omega)}\sqrt{|\triangle|}$$

*for a positive constant $C$ independent of $|\triangle|$.*

**Proof.** Since $\mathcal{S} \subset W^{1,1}(\Omega)$, we have $E(u_f) \le E(S_f)$. Also $\tilde{s} \in \mathcal{S}$ implies $E(S_f) \le E(\tilde{s})$. By Lemmas 3.3 and 3.5, we have

$$E(u_f) \le E(S_f) \le E(\tilde{s}) \le E(u_f^\epsilon) + err(|\triangle|, \epsilon) \le E(u_f) + err_\epsilon + err(|\triangle|, \epsilon).$$

For each triangulation $\triangle$, we choose $\epsilon = \sqrt{|\triangle|}$ which ensures $|\triangle|/\epsilon \to 0$. Thus, the above error terms go to zero as $|\triangle| \to 0$. By Lemma 3.2, $S_f$ converges to $u_f$ in $L^2$ norm.

When $u_f \in W^{1,2}(\Omega)$, we have $err_\epsilon \le \epsilon C|u_f|_{W^{1,2}(\Omega)}$ and $err(|\triangle|, \epsilon) \le C\sqrt{|\triangle|}|u_f|_{W^{1,2}(\Omega)}$ as we trivially have $|u_f|_{W^{1,1}(\Omega)} \le C|u_f|_{W^{1,2}(\Omega)}$ with positive constant $C$ dependent only on $A_\Omega$. These complete the proof. ■

**Remark 3.1** *It is interesting to know if $S_f$ approximates $u_f$ when $u_f \in BV(\Omega)\backslash W^{1,1}(\Omega)$.*

## 3.3 A Fixed Point Algorithm and Its Convergence

The following iterations will be used to approximate $S_f$.

**Algorithm 3.1** *Given $u^{(k)}$, we find $u^{(k+1)} \in \mathcal{S}$ such that*

$$\int_\Omega \frac{\nabla u^{(k+1)} \cdot \nabla \phi_j}{\sqrt{1 + |\nabla u^{(k)}|^2}} dx + \frac{1}{\lambda A_\Omega}\int_\Omega u^{(k+1)}\phi_j dx = \frac{1}{\lambda A_\Omega}\int_\Omega f\phi_j dx, \quad \text{for all } j = 1, ..., n. \tag{36}$$

We first show that the above iteration is well defined. Since $u^{(k+1)} \in \mathcal{S}$, it can be written as $u^{(k+1)} = \sum_i^n c_i^{(k+1)}\phi_i$. Plugging it in (36), we have

$$\sum_i^n c_i^{(k+1)}\left(\int_\Omega \frac{\nabla\phi_i \cdot \nabla\phi_j}{\sqrt{1 + |\nabla u^{(k)}|^2}} dx + \frac{1}{\lambda A_\Omega}\int_\Omega \phi_i\phi_j dx\right) = \frac{1}{\lambda A_\Omega}\int_\Omega f\phi_j dx, \quad j = 1, ..., n. \tag{37}$$

Denote by

$$D^{(k)} \quad := \quad (d_{i,j}^{(k)})_{N\times N} \text{ with } d_{i,j}^{(k)} = \lambda\int_\Omega \frac{\nabla\phi_i \cdot \nabla\phi_j}{\sqrt{1 + |\nabla u^{(k)}|^2}} dx,$$

$$\begin{aligned} M &:= (m_{i,j})_{N\times N} \text{ with } m_{i,j} = \frac{1}{A_\Omega}\int_\Omega \phi_i\phi_j dx, \\ \mathbf{v} &:= (v_j, j = 1, \cdots, N) \text{ with } v_j = \frac{1}{A_\Omega}\int_\Omega f\phi_j dx. \end{aligned}$$

Then to solve equation of (37) is equivalent to solving the equation

$$(D^{(k)} + M)\mathbf{c}^{(k+1)} = \mathbf{v}, \tag{38}$$

where $\mathbf{c}^{(k+1)} = [c_1^{(k+1)}, c_2^{(k+1)}, ..., c_n^{(k+1)}]^T$.

**Lemma 3.6** *(38) has a unique solution* $\mathbf{c}^{(k+1)}$.

**Proof.** It is easy to prove $D^{(k)}$ is semi-positive definite and $M$ is positive definite because, for any nonzero $\mathbf{c} = (c_i)_n$,

$$\mathbf{c}^T D^{(k)}\mathbf{c} = \lambda\int_\Omega \frac{|\sum_i^n c_i\nabla\phi_i|^2}{\sqrt{1+|\nabla u^{(k)}|^2}}dx \geq 0,$$

and

$$\mathbf{c}^T\ M\ \mathbf{c} = \frac{1}{A_\Omega}\int_\Omega |\sum_i^n c_i\phi_i|^2 dx > 0.$$

Moreover $(D^{(k)} + M)$ is also positive definite, and hence invertible. So (38) has a unique solution. ■

**Lemma 3.7** $\{u^{(k)}, k = 1, 2, \cdots\}$ *are bounded in* $L^2$ *norm by* $\|f\|_2$ *for all* $k > 0$. *That is,*

$$\|u^{(k+1)}\|_2 \leq \|f\|_2. \tag{39}$$

*Also, there exists a positive constant* $C$ *dependent on* $\beta$ *and* $|\triangle|$ *such that*

$$\|\nabla u^{(k+1)}\|_2 \leq C\|f\|_2.$$

**Proof.** Multiply $(\mathbf{c}^{(k+1)})^T$ to both hand-side of (38), we have

$$\lambda\int_\Omega \frac{|\nabla u^{(k+1)}|^2}{\sqrt{1+|\nabla u^{(k)}|^2}}dx + \frac{1}{A_\Omega}\int_\Omega |u^{(k+1)}|^2 dx = \frac{1}{A_\Omega}\int_\Omega f u^{(k+1)} dx. \tag{40}$$

Since the first term of (40) are nonnegative, we have

$$\|u^{(k+1)}\|_2^2 \leq \frac{1}{A_\Omega}\int_\Omega f u^{(k+1)} \leq \|f\|_2\|u^{(k+1)}\|_2 \tag{41}$$

which yields

$$\|u^{(k+1)}\|_2 \leq \|f\|_2,$$

and hence $\|u^{(k+1)}\|_2$ is bounded if $f \in L^2(\Omega)$. The second part of the results of Lemma 3.7 follows straightforwardly by using Markov's inequality in Theorem 2.1. ■

Next we need to show that the iterative algorithm above converges. We need the following inequality. Note that the proof of the inequality is different from the one in Lemma 3.2. The reason is that $u^{(k+1)}$ is not a minimizer of $E(u)$ in $\mathcal{S}$. Thus the technique of the sub-differentiation can not be applied here. We have to give a different proof.

**Lemma 3.8** *If* $u^{(k+1)}$ *is the solution of our Algorithm 3.1, then the following inequality holds*

$$\|u^{(k)} - u^{(k+1)}\|^2 \leq 2\lambda A_\Omega(E(u^{(k)}) - E(u^{(k+1)})). \tag{42}$$

**Proof.** First of all we use (36) to have

$$\frac{1}{\lambda A_\Omega}\int_\Omega (f-u^{(k+1)})(u^{(k)}-u^{(k+1)})dx = \int_\Omega \frac{\nabla u^{(k)}\cdot\nabla u^{(k+1)}}{\sqrt{1+|\nabla u^{(k)}|^2}}dx - \int_\Omega \frac{|\nabla u^{(k+1)}|^2}{\sqrt{1+|\nabla u^{(k)}|^2}}dx$$

since $u^{(k)}-u^{(k+1)}$ is a linear combination of $\phi_j, j=1,\cdots,n$. Then the following inequality follows.

$$\frac{1}{\lambda A_\Omega}\int_\Omega (f-u^{(k+1)})(u^{(k)}-u^{(k+1)})dx \le \int_\Omega \frac{|\nabla u^{(k)}|^2}{2\sqrt{1+|\nabla u^{(k)}|^2}}dx - \int_\Omega \frac{|\nabla u^{(k+1)}|^2}{2\sqrt{1+|\nabla u^{(k)}|^2}}dx. \tag{43}$$

Now we are ready to prove (42). The difference between $E(u^{(k)})$ and $E(u^{(k+1)})$ is

$$\begin{aligned}
& E(u^{(k)}) - E(u^{(k+1)}) \\
= & \int_\Omega \sqrt{1+|\nabla u^{(k)}|} - \sqrt{1+|\nabla u^{(k+1)}|^2}dx + \frac{1}{2\lambda A_\Omega}\int_\Omega |u^{(k)}-f|^2 - |u^{(k+1)}-f|^2 dx \\
= & \int_\Omega \sqrt{1+|\nabla u^{(k)}|} - \sqrt{1+|\nabla u^{(k+1)}|^2}dx + \frac{1}{2\lambda A_\Omega}\int_\Omega (u^{(k)}-u^{(k+1)})(u^{(k)}+u^{(k+1)}-2f)dx \\
= & \int_\Omega \sqrt{1+|\nabla u^{(k)}|} - \sqrt{1+|\nabla u^{(k+1)}|^2}dx + \int_\Omega \frac{1}{\lambda A_\Omega}(u^{(k+1)}-f)(u^{(k)}-u^{(k+1)}) \\
& + \frac{1}{2\lambda A_\Omega}\int_\Omega |u^{(k)}-u^{(k+1)}|^2 dx
\end{aligned}$$

which yields the result of this lemma since the first two terms in the last equation above is not negative. Indeed, by applying (43), we have

$$\begin{aligned}
& \int_\Omega \sqrt{1+|\nabla u^{(k)}|} - \sqrt{1+|\nabla u^{(k+1)}|^2}dx + \frac{1}{\lambda A_\Omega}\int_\Omega (u^{(k+1)}-f)(u^{(k)}-u^{(k+1)}) \\
\ge & \int_\Omega \sqrt{1+|\nabla u^{(k)}|^2} - \sqrt{1+|\nabla u^{(k+1)}|^2}dx - \int_\Omega \frac{|\nabla u^{(k)}|^2}{2\sqrt{1+|\nabla u^{(k)}|^2}}dx + \int_\Omega \frac{|\nabla u^{(k+1)}|^2}{2\sqrt{1+|\nabla u^{(k)}|^2}}dx \\
= & \int_\Omega \frac{2+|\nabla u^{(k)}|^2+|\nabla u^{(k+1)}|^2}{2\sqrt{1+|\nabla u^{(k)}|^2}} - \sqrt{1+|\nabla u^{(k+1)}|^2}dx \\
\ge & \int_\Omega \frac{\sqrt{1+|\nabla u^{(k)}|^2}\sqrt{1+|\nabla u^{(k+1)}|^2}}{\sqrt{1+|\nabla u^{(k)}|^2}} - \sqrt{1+|\nabla u^{(k+1)}|^2}dx = 0.
\end{aligned}$$

We have thus established the proof. ■

We are ready to show the convergence of $u^{(k)}$ to the minimizer $S_f$.

**Theorem 3.2** *The sequence $\{u^{(k)}, k=1,2,\cdots,\}$ obtained from Algorithm 3.1 converges to the true minimizer $S_f$.*

**Proof.** By Lemma 3.7, the sequence $\{u^{(k)}, k=1,\cdots,\}$ is bounded. Actually, we know $\|u^{(k)}\|_2 \le \|f\|_2$. So there must be a convergent subsequence $\{u^{(n_j)}, n_1<n_2<\cdots<\}$. Suppose $u^{(n_j)}\to\bar{u}$. By Lemma 3.8, we see $\{E(u^{(k)}), k=1,2,\cdots,\}$ is a decreasing sequence and bounded below, so $\{E(u^{(k)})\}$ is convergent as well as any subsequence of it. We use Lemma 3.8 to have

$$\begin{aligned}
\|u^{(n_j+1)}-\bar{u}\|_2^2 &\le 2\|u^{(n_j+1)}-u^{(n_j)}\|_2^2 + 2\|u^{(n_j)}-\bar{u}\|_2^2 \\
&\le 4\lambda A_\Omega(E(u^{(n_j)})-E(u^{(n_j+1)})) + 2\|u^{(n_j)}-\bar{u}\|_2^2 \to 0,
\end{aligned}$$

which implies $u^{(n_j+1)}\to\bar{u}$.

According to Markov's inequality, i.e. Theorem 2.1, we have

$$\int_\Omega |\nabla u^{(n_j)} - \nabla \bar{u}|^2 dx \le \frac{\beta^2}{|\triangle|^2} \int_\Omega |u^{(n_j)} - \bar{u}|^2 dx. \tag{44}$$

It follows from the convergence of $u^{(n_j)} \to \bar{u}$ that $\nabla u^{(n_j)} \to \nabla \bar{u}$ in $L^2$ norm as well. Replacing $u^{(n_j)}$ by $u^{(n_j+1)}$ above, we have $\nabla u^{(n_j+1)} \to \nabla \bar{u}$ too by the convergence of $u^{(n_j+1)} \to \bar{u}$. As $u^{(n_j)}$, $u^{(n_j+1)}$ and $\bar{u}$ are spline functions in $\mathcal{S}$. The convergence of $u^{(n_j)}$ and $u^{(n_j+1)}$ to $\bar{u}$, respectively implies the coefficients of $u^{(n_j)}$ and $u^{(n_j+1)}$ in terms of the basis functions $\phi_j, j = 1, \cdots, N$ are convergent to the coefficients of $\bar{u}$, respectively.

Since $u^{(n_j+1)}$ solves the equations (36), we have

$$\int_\Omega \frac{\nabla u^{(n_j+1)} \cdot \nabla \phi_j}{\sqrt{1 + |\nabla u^{(n_j)}|^2}} dx = \int_\Omega \frac{f - u^{(n_j+1)}}{\lambda A_\Omega} \phi_i dx \tag{45}$$

for all $\phi_i, i = 1, \cdots, N$. Letting $j \to \infty$, we obtain

$$\int_\Omega \frac{\nabla \bar{u} \cdot \nabla \phi_i}{\sqrt{1 + |\nabla \bar{u}|^2}} dx = \int_\Omega \frac{f - \bar{u}}{\lambda A_\Omega} \phi_i dx \tag{46}$$

for all $i = 1, \cdots, N$. That is, $\bar{u}$ is a local minimizer. Since the functional is convex, a local minimizer is the global minimizer and hence, $\bar{u} = S_f$. Thus all convergent subsequences of $\{u^{(k)}\}$ converge to $S_f$. ■

# 4 Discrete Spline Minimizer $s_f$ and Its Properties

In this section we mainly discuss the properties of discrete spline minimizer $s_f$ of (10).

## 4.1 Existence, Uniqueness and Stability

Let us first discuss basic properties of the minimizer of (10). We begin with the following

**Lemma 4.1** *Suppose that the data sites $x_i, i = 1, \cdots, n$ satisfy the condition (16). Then the minimization problem (10) has one and only one solution.*

**Proof.** Mainly, we need to show that $E_d(u)$ is strictly convex under the condition in (16). Suppose that there are two minimizers $s_1$ and $s_2$ of (10). Then any convex combination $\alpha s_1 + (1-\alpha)s_2$ is also a minimizer since $E_d$ is convex. We claim that if $s_1(x_i, y_i) \neq s_2(x_i, y+i)$ for some $i$ between $1 \le i \le n$, then

$$E_d(\alpha s_1 + (1-\alpha)s_2) < \alpha E_d(s_1) + (1-\alpha) E_d(s_2).$$

Indeed, letting us say $s_1(x_n, y_n) \neq s_2(x_n, y_n)$,

$$(\alpha s_1(x_n, y_n) + (1-\alpha)s_2(x_n, y_n))^2 < \alpha (s_1(x_n, y_n))^2 + (1-\alpha)(s_2(x_n, y_n))^2.$$

Thus, $E_d(\alpha s_1 + (1-\alpha)s_2) < E_d(s_1)$. It is a contradiction. Therefore, we $s_1(x_i, y_i) = s_2(x_i, y_i), i = 1, \cdots, n$. Now we use the condition (16) to see $s_1 - s_2$ is a zero spline function. That is, $s_1 \equiv s_2$. This shows that $E_d$ is strictly convex over finite dimensional space $\mathcal{S}$. Thus, there exists a unique minimizer of the minimization (10). ■

Next we show that the discrete spline minimizer $s_f$ is stable. Let

$$\|f\|_d^2 = \frac{1}{n} \sum_{i=1}^n |f(x_i)|^2$$

be the norm for vector $f = (f(x_1), \cdots, f(x_n))^T$. Let $s_f \in \mathcal{S}$ be the solution of (10) associated with the given function $f$. Similarly, let $s_g \in \mathcal{S}$ be the minimizer of (10) associated with $g$. By using the same method in the proof of Lemma 3.1, we can prove

**Lemma 4.2** *The norm of the difference of spline functions $s_f$ and $s_g$ over discrete points $x_1, \cdots, x_n$ is bounded by the norm of the difference of $f$ and $g$ over the discrete points, i.e.*

$$\|s_f - s_g\|_d \leq \|f - g\|_d. \tag{47}$$

## 4.2 Numerical Algorithms and Their Convergence

We now study how to compute numerically the minimizer $s_f$ of (10). First of all, we shall definite a computational algorithm for $s_f$. Then we shall prove some properties of the iterative sequence. With these preparation, we shall prove that our numerical algorithm is convergent and iterative solutions converge to $s_f$.

**Algorithm 4.1** *Given $u^{(k)} \in \mathcal{S}$, we find $u^{(k+1)} \in \mathcal{S}$ such that*

$$\lambda \int_\Omega \frac{\nabla u^{(k+1)} \cdot \nabla \phi_j}{\sqrt{1 + |\nabla u^{(k)}|^2}} dx + \frac{1}{n} \sum_{i=1}^n u^{(k+1)}(x_i)\phi_j(x_i) = \frac{1}{n} \sum_{i=1}^n f(x_i)\phi_j(x_i), \quad \text{for all } j = 1, ..., n. \tag{48}$$

We can prove that the iterative algorithm is well defined if we assume the condition (16). Indeed, as above, we write $u^{(k+1)} = \sum_i^n c_i^{(k+1)} \phi_i$. Plugging it in (48), we have

$$\sum_i^n c_i^{(k+1)} \left( \lambda \int_\Omega \frac{\nabla \phi_i \cdot \nabla \phi_j}{\sqrt{1 + |\nabla u^{(k)}|^2}} dx + \frac{1}{n} \sum_{\ell=1}^n \phi_i(x_\ell)\phi_j(x_\ell) \right) = \frac{1}{n} \sum_{\ell=1}^n f(x_\ell)\phi_j(x_\ell), \quad j = 1, ...n. \tag{49}$$

These lead to the following system of equations

$$(D^{(k)} + \widetilde{M}) c^{(k+1)} = \widetilde{\mathbf{v}}, \tag{50}$$

where the matrix $\widetilde{M}$ and vector $\widetilde{\mathbf{v}}$ are slightly different from the matrix $M$ and the vector $\mathbf{v}$ above.

**Lemma 4.3** *Suppose that the data locations satisfy the condition (16). Then (50) has a unique solution $c^{(k+1)}$.*

**Proof.** We have seen that $D^{(k)}$ is semi-positive definite. We now show that $\widetilde{M}$ is positive defined. For any nonzero $\mathbf{c} = (c_i)_n$,

$$\mathbf{c}^T \ \widetilde{M} \ \mathbf{c} = \frac{1}{n} \sum_{\ell=1}^n |\sum_i^n c_i \phi_i(x_\ell)|^2 > 0.$$

Indeed, if the above term is zero, then for each triangle $t$, we have

$$F_1 \| \sum_i^n c_i \phi_i \|_{\infty,t} \leq \sum_{\ell=1}^n |\sum_i^n c_i \phi_i(x_\ell)|^2 = 0,$$

which implies that the spline function $\sum_i^n c_i \phi_i \equiv 0$ and hence, the coefficients $c_i$ are all zero. This is a contradiction. Thus, $\widetilde{M}$ is positive.

That is, $(D^{(k)} + \widetilde{M})$ is also positive definite, and hence invertible. So (38) has a unique solution. ■

Similarly, we can show that $u^{(k)}$ is bounded in the following sense:

**Lemma 4.4** *Suppose that the data locations satisfy the condition (16). Then $\{u^{(k)}\}$ are bounded for all $k > 0$. That is,*

$$\sum_{i=1}^n |u^{(k+1)}(x_i)|^2 \leq \sum_{i=1}^n |f_i|^2. \tag{51}$$

*In addition,*

$$\|\nabla u^{(k+1)}\|_2^2 \leq C \sum_{i=1}^{n} |f_i|^2,$$

*where $C$ is dependent on $\beta$ and $|\triangle|$.*

**Proof.** Multiply $(c^{(k+1)})^T$ to both hand-side of (38), we have

$$\lambda \int_\Omega \frac{|\nabla u^{(k+1)}|^2}{\sqrt{1+|\nabla u^{(k)}|^2}} dx + \frac{1}{n} \sum_{\ell=1}^{n} |u^{(k+1)}(x_\ell)|^2 = \frac{1}{n} \sum_{\ell=1}^{n} f_\ell u^{(k+1)}(x_\ell). \tag{52}$$

By Cauchy-Schwarz's inequality, we have

$$\sum_{\ell=1}^{n} f_\ell u^{(k+1)}(x_\ell) \leq \frac{1}{2} \sum_{\ell=1}^{n} |f_\ell|^2 + \frac{1}{2} \sum_{\ell=1}^{n} |u^{(k+1)}(x_\ell)|^2.$$

It follows

$$\lambda \int_\Omega \frac{|\nabla u^{(k+1)}|^2}{\sqrt{1+|\nabla u^{(k)}|^2}} dx + \frac{1}{2n} \sum_{\ell=1}^{n} |u^{(k+1)}(x_\ell)|^2 \leq \frac{1}{2n} \sum_{\ell=1}^{n} |f_\ell|^2. \tag{53}$$

Thus we have the first part of Lemma 4.4. To see the second part, we prove the maximum norm $\|\nabla u^{(k+1)}\|_{\infty,\Omega}$ is bounded by the right-hand side of (51). Indeed, by Theorem 2.1, we have

$$\|\nabla u^{(k+1)}\|_{\infty,\Omega} \leq \frac{C}{|\triangle|} \|u^{(k+1)}\|_{\infty,\Omega}.$$

As the maximum norm of $u^{(k+1)}$ is achieved at a triangle $t \in \triangle$, we use the condition (16) to see

$$\|u^{(k+1)}\|_{\infty,\Omega} \leq \frac{1}{F_1} \left( \sum_{\ell=1}^{n} |u^{(k+1)}(x_\ell)|^2 \right)^{1/2} \leq \frac{1}{F_1} \left( \sum_{\ell=1}^{n} |f_\ell|^2 \right)^{1/2}.$$

It follows that the second part of Lemma 4.4 is true. ■

Similarly, letting $u^{(k)}$ be the sequence from Algorithm 4.1, we can show the convergence of $u^{(k)}$ to the minimizer $s_f$. The proof of the following theorem is similar to Theorem 3.2 and is left to the interested reader.

**Theorem 4.1** *Suppose that the data sites $x_i, i = 1, \cdots, n$ satisfy the condition in (16). Then the sequence $\{u^{(k)}\}$ obtained from Algorithm 4.1 converges to the true minimizer $s_f$.*

# 5 Numerical Results

We have implemented our bivariate spline approach in MATLAB and performed several image enhancement experiments: image denoising, image inpainting, image rescaling and wrinkle removal. We shall briefly explain how to choose a polygonal domain, how to triangulate a polygonal domain, how to use a bivariate spline space in following subsections. After these, we report our numerical results.

## 5.1 Image Segmentation

First of all, let us briefly explain how to choose a polygonal domain. For image inpainting and wrinkle reduction, we simply choose a polygonal domain of interest by hand. For image rescaling, the polygonal domain is the image domain. For image denoising, we use the active contour method proposed in [9] to choose polygonal domains. The basic idea is to evolve a closed curve to detect objects in an image, subject to the minimization of an energy defined in (54) below. For simplicity, let us assume that the image $u$ is formed by two regions of approximatively piecewise-constant intensities of two distinct values $u_1$ and $u_2$ and they are separated by a contour $C_0 := \{x : \phi(x) = 0, x \in \Omega\}$. The goal is to find the "fittest" boundary $C$ which best approximates $C_0$. One numerically computes an approximation $C$ of $C_0$. Then the image is segmented into two distinguished regions: one is inside $C$ and the other is outside $C$. In [9] the research considered the following minimization functional on $C$:

$$F(C) = \mu Length(C) + \nu Area(inside\ C) + \int_{inside(C)} |u(x) - u_1|^2 dxdy + \int_{outside(C)} |u(x) - u_2|^2 dx, \quad (54)$$

where $C$ is a variable curve represented by level set $\{x : \phi(x) = 0, x \in \Omega\}$. In our computation, $\mu = \nu = 1/2$ and $\phi$ is approximated by a piecewise constant function over $\Omega$. Here $u_1 := u_1(C)$ and $u_2 := u_2(C)$ are the average values of the image inside and outside $C$, respectively, which are defined as

$$u_1 = \int_{inside(C)} u(x, y)dxdy \text{ and } u_2 = \int_{outside(C)} u(x, y)dxdy.$$

Then $C_0$ is the minimizer of the fitting term

$$\inf_C F(C).$$

To deal with complicated images with more than two distinguished regions, we have to apply the active contour segmentation method iteratively. We implement this method based on numerical integration with equally-spaced grids. Figure 1 gives an example which shows the process of the iterations. Figure (a) is the original image to be segmented; (b) is the resulting image after the first iteration of the active contour method, the original images is divided into two regions(black and white); (c) the black region in (b) is divided into another two regions(gray and white) by one more iteration of the active contour method; (d) shows combining the results of two iterations by assigning different colors to separate regions; (e) is the triangulation based on the segmentations result from (d).

To help the performance of the above segmentation, we use the standard discrete Perona-Malik (PM) model with diffusivity function $c(s) = 1/\sqrt{1+s}$ to reduce the noises first. With this relatively clean image, we apply for the iterative active contour method to separate an image into many regions. Then we obtain the triangulations as shown in Fig. 5.1.

## 5.2 Triangulation

We mainly use the standard Delaunay triangulation algorithm to find a triangulation of a polygon. A key ingredient is to choose boundary points as equally-spaced as possible and points inside the polygon as evenly-distributed as possible. If some points are clustered near the boundary of the polygon, we have to thin a few point off. In addition, we check the triangles from the Delaunay triangulation method to see which one is outside of the domain and delete such triangles. Triangles in triangulations from our MATLAB code have almost uniform in size and in area.

## 5.3 How to Use Bivariate Splines

Let us explain how to implement the bivariate splines as locally supported basis functions are hard to construct. We mainly use the ideas in [2]. That is, fixed $r \geq 0$ and $d > 0$, we express the polynomial piece

of each spline function $s$ over a triangle $T \in \triangle$ in B-form. That is, $s = \sum_{T\in\triangle}\sum_{i+j+k=d} c_{T,ijk}B_{T,ijk}$ is expressed in a discontinuous function over $\triangle$. Then we add smoothness conditions including continuous conditions as side constrains. I.e., let $H$ be the smoothness matrix such that $H\mathbf{c} = 0$ for $\mathbf{c} = (c_{T,ijk}, T \in \triangle, i+j+k = d)^T$ if and only if $s \in S_d^r(\triangle)$. See [Lai and Schumaker'07] and [2] for B-form and constructing $H$. We iteratively solve $S_f$ in the following system of nonlinear equations:

$$\int_\Omega \frac{\nabla S_f \cdot \nabla \phi_m}{\sqrt{1+|\nabla S_f|^2}} dx + \frac{1}{\lambda}\frac{1}{A_\Omega}\int_\Omega (S_f - f)\phi_m dx = 0 \tag{55}$$

subject to the smoothness constrains $S_f \in S_d^r(\triangle)$, where $\phi_m$ is one of discontinuous functions $B_{T,ijk}$ which is defined only on $T$ and $i+j+k = d$. This system can be solved by using the iterative algorithm in [4]. Similar for the discrete spline minimizer $s_f$. We always use the penalized least squares splines defined in §2 as an initial $S_f$ to start the iteration. Each iteration will reduce the area of fitting spline surface. When the fitting spline surface areas become stable, we stop the iterations. The computational method works for any $r$ and $d$ with $d > r$. In our experiments, we use $r = 1$ and $d \geq 3$. In Fig. 2, we demonstrate that our discrete minimal surface area spline fit is better than the penalized least square spline fit. However, in terms of peak signal to noise ratio, a penalized least squares spline fit can give better denoised image values sometimes.

## 5.4 Numerical Results

**Example 5.1 (Image Denoising)** *Image denoising is a standard procedure for image enhancement. We shall use the minimal surface area approach discussed in this paper to reduce the noises from a noised image. Let us consider a standard image Peppers and add a Gaussian noise* $20N(0,1)$ *to get a noised image* $L$*. We first use the standard discrete Perona-Malik (PM) model with diffusivity function* $c(s) = 1/\sqrt{1+s}$ *to reduce the noises of* $L$*. Of course, one can use other favorable denoising method. Then we run our image segmentation method discussed above to decompose the image into several regions of interest for further reduction of noises. In Fig. 2, several triangulations of the image* $L$ *are shown. It takes about 1 minute to get all triangulations done. There are 8 regions and 8 triangulations as shown. We apply our minimal surface area spline (MSA) approach to further remove the noises from these regions with penalized least squares spline (PLS) fits as initial fitting splines. We use bivariate splines of smoothness is* 1 *and the degree* $d = 6$*. In the following table we show the peak signal to noises ratio over each region.*

**Table 1. PSNR over each region by PM, PLS, MSA methods**

| | *PM* | *PLS* | *MSA* |
|---|---|---|---|
| *Region 1* | *30.7756* | *30.7852* | *30.7654* |
| *Region 2* | *29.9161* | *29.9158* | *29.9109* |
| *Region 3* | *28.8445* | *28.8470* | *28.9952* |
| *Region 4* | *30.9243* | *30.9200* | *30.8882* |
| *Region 5* | *31.6307* | *31.6296* | *31.6989* |
| *Region 6* | *33.0744* | *33.0961* | *33.1167* |
| *Region 7* | *33.3464* | *33.3430* | *33.5832* |
| *Region 8* | *32.4490* | *32.4959* | *32.5882* |
| **final PSNR** | *31.9459* | *31.9727* | *32.0163* |

*In Fig. 3, we show a noised image (using Gaussian noises* $20N(0,1)$*), a denoised image by using our approach, an exact image and a denoised image by using the discrete PM model. We put all four images in one page so that they can be compared to demonstrate that our approach works very well, where the standard peak signal to noise ratio is used. The computational time is about 2 minutes.*

*From Fig. 3 we can see that the denoised image by our approach is smooth in the regions where our approach is applied and they are even smoother than the original exact image. The denoised image by the Perona-Malik approach looks bumpy in a few local regions. For the whole image, our result is demonstrated as in Fig. 4.*

**Example 5.2 (Image Inpainting)** *In Fig. 5, we show a damaged image and the recovered image by using the minimal surface area fitting splines to recover the loss image data values from the damaged image. In the computation, we used the triangulations in Fig. 6.*

**Example 5.3 (Image Scaling)** *We apply the minimum surface area fitting splines to image rescaling and compared our method to the bicubic and bilinear interpolation methods provided by MATLAB function "imresize". In Fig. 7, the two images showed in the first column(not in actual size) are scaled by 10. The first original image is of dimension* $18 \times 28$*, and the second one is of* $24 \times 15$*. One can notice that both the bicubic and bilinear interpolation methods lead to the gibbs discontinuity effect at the edges of the two images, while our approach barely show any such effect.*

**Example 5.4 (Wrinkle Removal)** *Finally we present a wrinkle removal experiment. We are interested in reducing some wrinkles from a human face. We identify a couple of regions of interest near eyes and cheeks and apply our bivariate spline approach over each region. In Fig. 8, two images are shown. The human face on the right is clearly enhanced in the areas near eyes and cheeks. Fig. 9 shows the enlarged pictures of the 4 positions where wrinkles are removed.*

# References


[1] Acar R., C.R. Vogel (1994): Analysis of bounded variation penalty methods for ill-posed problems, Inverse Problems, 10, 1217-1229.

[2] G. Awanou, M. J. Lai, and P. Wenston, *The multivariate spline method for numerical solution of partial differential equations and scattered data interpolation*, in Wavelets and Splines: Athens 2005, edited by G. Chen and M. J. Lai, Nashboro Press, Nashville, TN, 2006, 24–74.

[3] G. Aubert and P. Kornprobst, *Mathematical Problems in Image Processing*, Springer, 2006.

[4] G. Awanou and M. J. Lai, On the convergence rate of the augumented Lagrangian algorithm for the nonsymmetric saddle point problem, J. Applied Numerical Mathematics, (54) 2005, 122–134.

[5] F. Ciarlet, The Finite Element Method for Elliptic Problems, North- Holland, Amsterdam, New York, 1978.

[6] A. Chambolle, An algorithm for total variation minimization and applications, Journal of Mathematical Imaging and Vision, **20** (2004), Issue 1-2, 89-97.

[7] Chambolle, A., and Lions, P.-L.: Image recovery via total variation minimization and related problems, *Numer. Math.* **76**(2) (1997), 167-188.

[8] A. Chambolle, R. A. DeVore, N. Lee, and B. J. Lucier, Nonlinear wavelet image processing: variational problems, compression, and noise removal through wavelet shrinkage, IEEE Trans. Image Process., **7**(1998), 319–335.

[9] T. Chan, L. A. Vese, Active Contour Without Edge, IEEE Transactions on Image Processing, VOL. 10, No.2, 2001, 266-277.

[10] Chan, T. F.; Vese, L. A. Active contour and segmentation models using geometric PDE's for medical imaging, Geometric methods in bio-medical image processing, 6375, Math. Vis., Springer, Berlin, 2002,

[11] D. C. Dobson and C. R. Vogel. Convergence of an iterative method for total variation denoising. SIAM J. Numer. Anal., 34(1997), 1779–1791.

[12] Duval, V. J.-F. Aujol and L. Vesse, A projected gradient algorithm for color image decomposition, CMLA Preprint 2008–21.

[13] I. Ekeland and R. Temam, Convex Analysis and Variational Problem, Cambridge University Press, 1999.

[14] L. C. Evans, Partial Differential Equations, American Mathematical Society, 2002, pp 629-631.

[15] X. Feng and A. Prohl. Analysis of total variation flow and its finite element approximations, Math. Mod. Num. Anal., 37(2003) 533–556, 2003.

[16] X. Feng, M. von Oehsen, and A. Prohl. Rate of convergence of regularization procedures and finite element approximations for the total variation flow, Numer. Math., 100(2005), 441–456.

[17] M. von Golitschek, M. J. Lai, L. L. Schumaker, *Error bounds for minimal energy bivariate polynomial splines*, Numer. Math. 93(2002), 315–331.

[18] M. von Golitschek and L. L. Schumaker, *Bounds on projections onto bivariate polynomial spline spaces with stable local bases*, Const. Approx. 18(2002), 241–254.

[19] M. von Golitschek and L. L. Schumaker, *Penalized least squares fitting*, Serdica 18 (2002), 1001–1020.

[20] M.-J. Lai, Multivariate splines for data fitting and approximation, Approximation Theory XII, San Antonio, 2007, edited by M. Neamtu and L. L. Schumaker, Nashboro Press, 2008, Brentwood, TN, pp. 210–228.

[21] M. -J. Lai and L. L. Schumaker, Approximation power of bivariate splines, Advances in Comput. Math., 9(1998), pp. 251–279.

[22] M. -J. Lai and L. L. Schumaker, *Spline Functions on Triangulations* , Cambridge University Press, 2007.

[23] M. -J. Lai and L. L. Schumaker, *Domain decomposition technique for scattered data interpolation and fitting*, SIAM J. Numerical Analysis, 47(2009), 911-928.

[24] P. Parona and J. Malik, Scale-Space and Edge Detection Using Anisotropic Diffusion, 12 (1990), pp. 629–639.

[25] L. Rudin, Osher, S., Fatemi, E., Nonlinear total variation based noise removal algorithms. Physica D 60 (1992), 259-268.

[26] E. M. Stein, Singular Integrals and Differentiability Properties of Functions, Princeton University Press, 1970.

[27] X.-C.-Tai et al., eds., *Scale Space and Variational Methods in Computer Vision*, Lecture Notes in Computer Science, Vol. 5567, Springer Berlin, Heidelberg, 2009.

[28] L. Vese, A study in the BV space of a denoising-deblurring variational problem, Applied Maht. Optim, 44(2001), 131–161.

[29] C. R. Vogel and M. E. Oman, Iterative methods for total variation denoising. SIAM J. Sci. Comput. 17 (1996), no. 1, 227-238,

[30] J. Wang and Lucier, B., Error bounds for finite-difference methods for Rudin-Osher-Fatemi image smoothing, submitted, 2009.

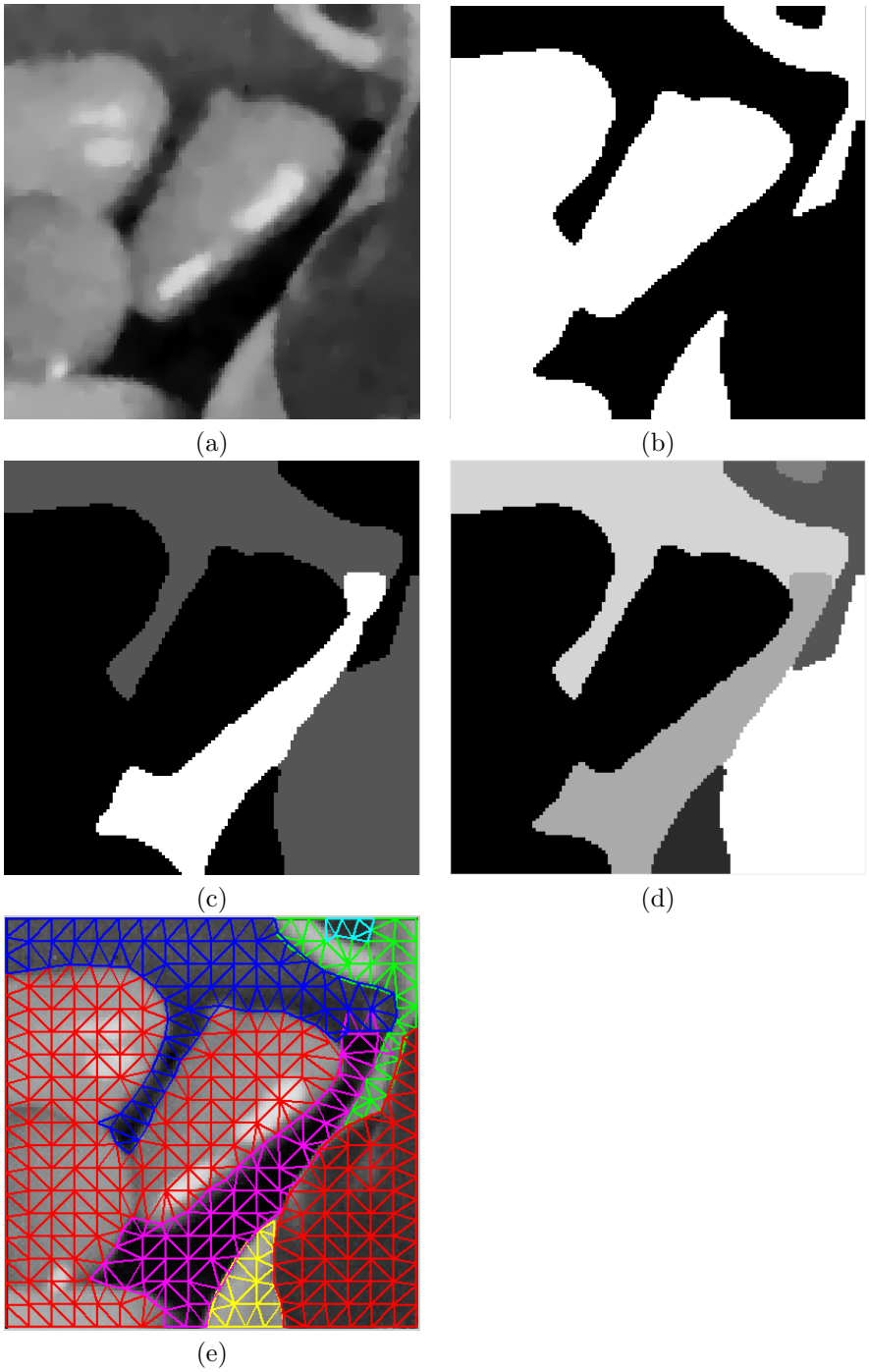

Figure 1: Iterative Active Contours (a)–(d) and Triangulations of 8 regions (e).

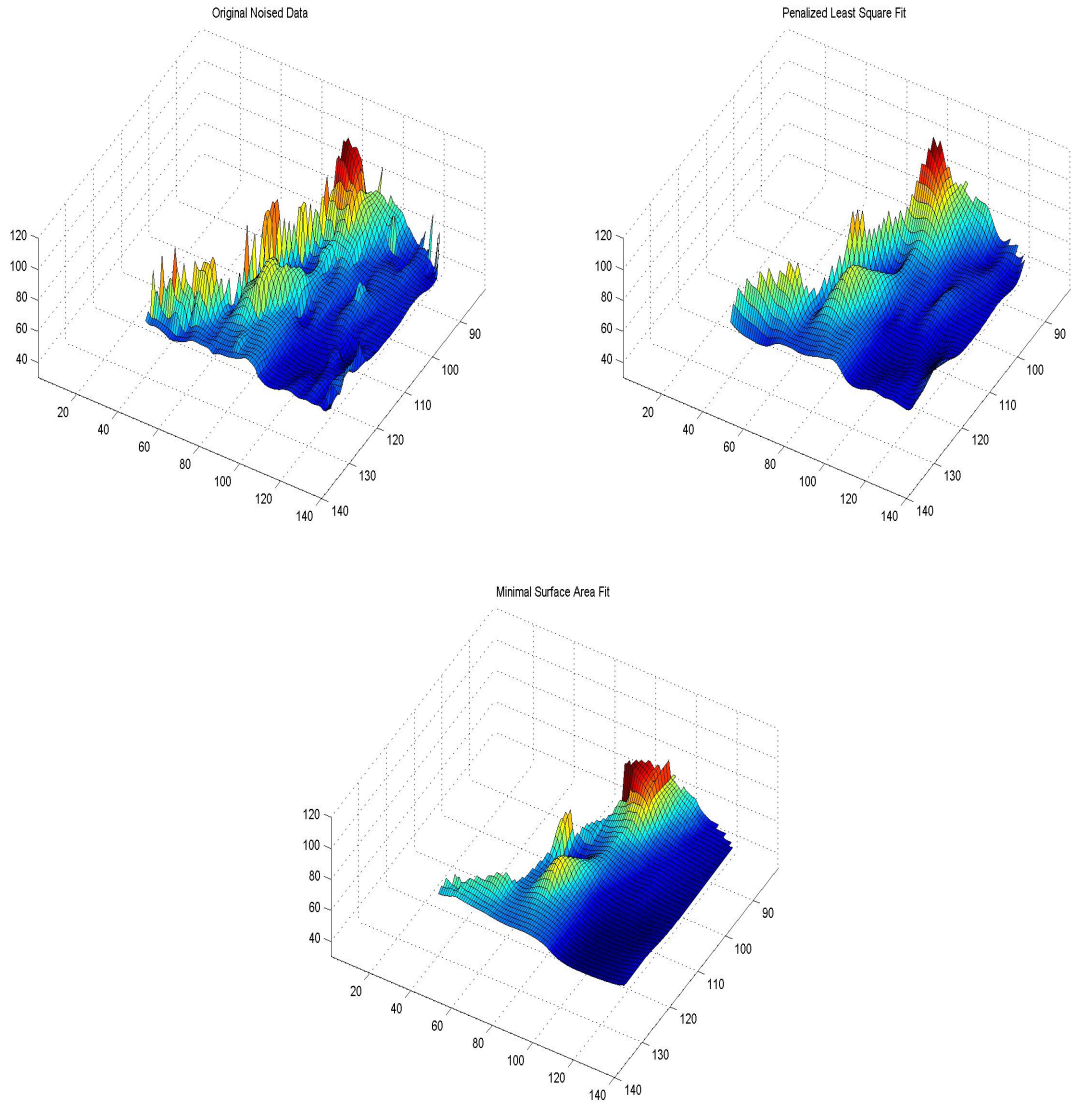


Figure 2: A noised data values, a penalized least squares spline fit and a minimal surface area spline fit.

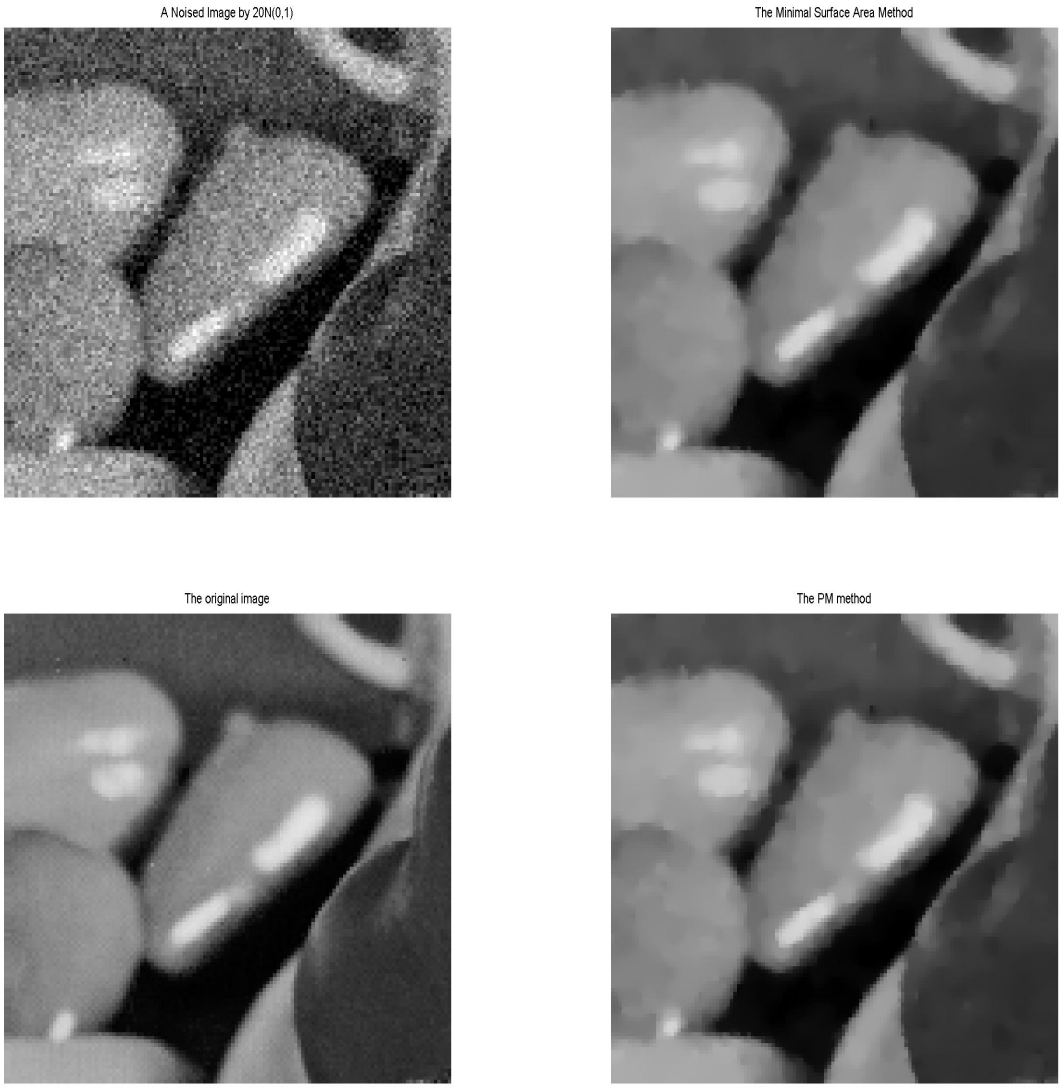


Figure 3: A noised peppers image and the denoised image by our approach(top row) and the exact image and denoised images by the Perona-Malik method(bottom row).


Figure 4: The denoised image by our approach (left) and the denoised image by the Perona-Malik method(right) from a noised image with additive Gaussian noise of $\sigma = 20$. $d = 7$ and $r = 1$ are used in our computation.


Figure 5: Inpainting domain are marked by two blacked words. $d = 3$ and $r = 1$ are used in our computation.

Figure 6: These two triangulations are used in our computation.

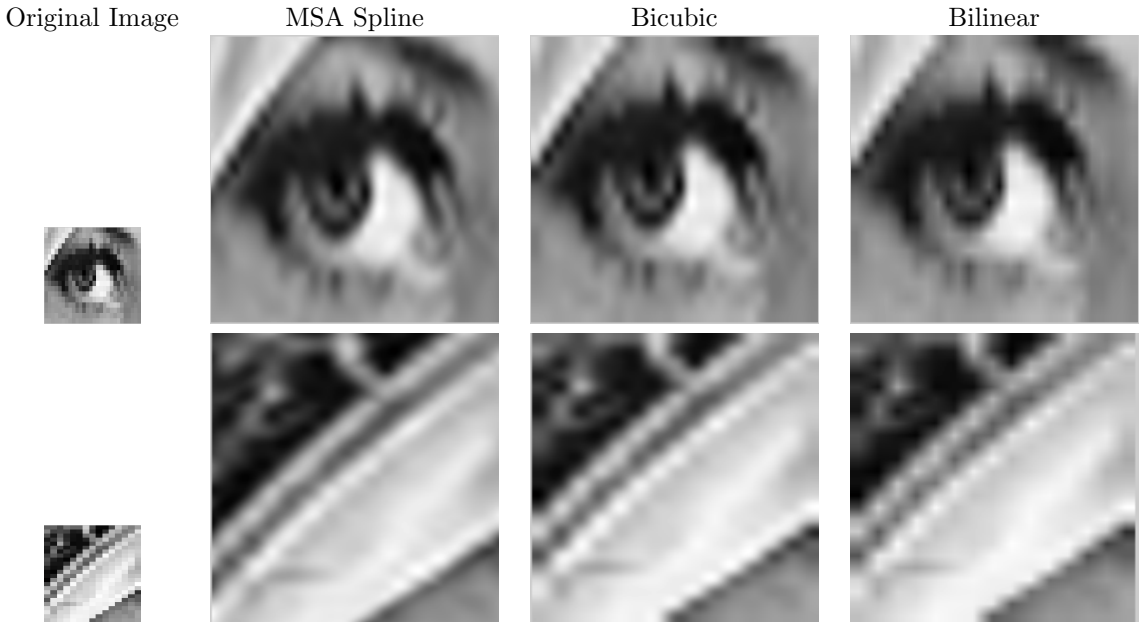


Figure 7: Images are scaled by 10 by using our spline method($d = 7, r = 1$), Bicubic and Bilinear interpolation respectively.

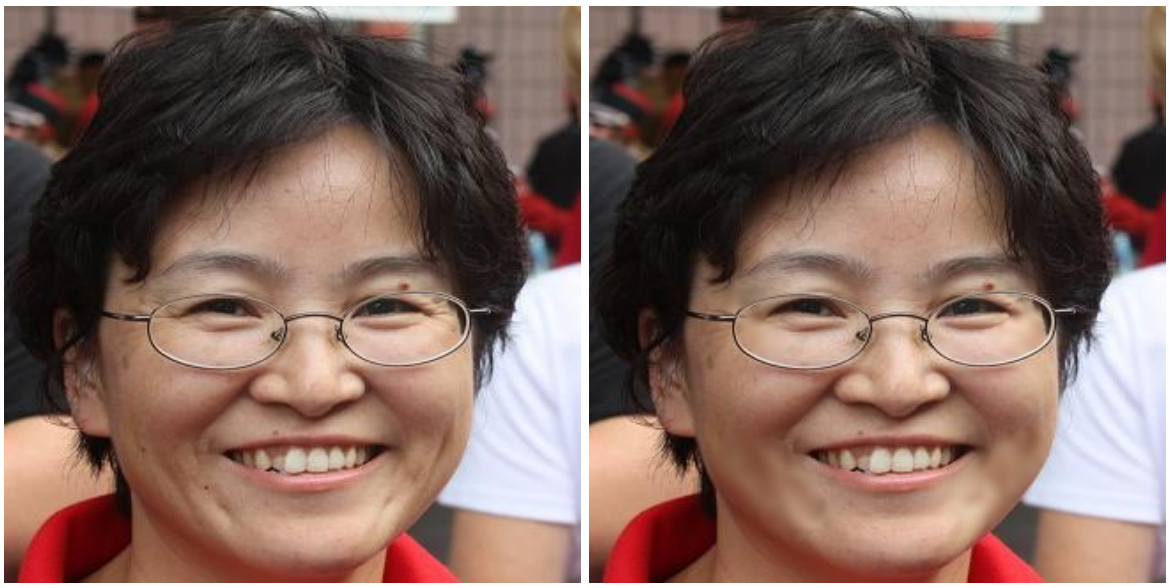

Figure 8: A face with wrinkles on the left and the face with reduced wrinkles on the right. We use $d = 3$ and $r = 1$ in our computation.

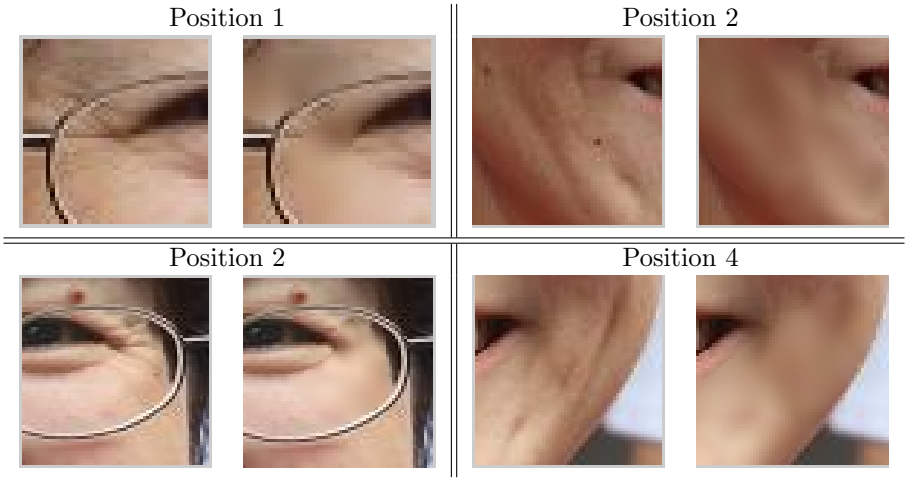


Figure 9: Enlarged pictures of 4 positions where wrinkles are removed.